

## Chapter 4

# IMIDAZOLIUM-BASED IONIC LIQUID FUNCTIONAL MATERIALS AND THEIR APPLICATION TO ELECTROANALYTICAL CHEMISTRY

**Yuanjian Zhang, Yanfei Shen, and Li Niu**

*State Key Laboratory of Electroanalytical Chemistry,*

*Changchun Institute of Applied Chemistry,*

*Graduate School of the Chinese Academy of Sciences,*

*Chinese Academy of Sciences, Changchun 130022, P. R. China*

[lniu@ciac.jl.cn](mailto:lniu@ciac.jl.cn)

### 4.1 INTRODUCTION

Ionic liquids (ILs) are low-melting-point salts, thus forming liquids that consist only of cations and anions. They are often applied to any compounds that have a melting point less than 100°C. The first useful IL, ethylammonium nitrate, described by Walden, seems to have generated little interest; it was not until the 1980s that the physical and chemical properties of this salt were investigated [1]. This was followed by the discovery that several tetraalkylammonium salts form air- and moisture-stable

---

*Electrochemical Nanofabrication: Principles and Applications*

Edited by Di Wei

Copyright © 2012 by Pan Stanford Publishing Pte. Ltd.

[www.panstanford.com](http://www.panstanford.com)

ILs of interesting properties. For the overall environmental impact and economics, they were employed as solvents for electrochemistry [2–8], analytical chemistry [9], chemical synthesis [10–14], liquid/liquid separations and extractions [15–17], dissolution [18–20], catalysis [21–25], and polymerization [26]. In electrochemistry, they show relatively wide potential window and high conductivity and allow studies to be undertaken without additional supporting electrolyte [27]. Thus various applications including in electrodeposition, electropolymerization, capacitors, Li-ion batteries, and solar cell have been intensive investigated [28]. ILs have also offered many opportunities in electroanalytical chemistry [29]. Particularly, some task-specific ILs have also been designed because the structures and properties of ILs can be easily tuned by selecting proper combination of organic cations and anions. Equally importantly, these unique properties of ILs could be extended to the concept of task-specific IL-materials. No longer as simple green solvents, it would greatly expand the potential application of ILs. As excellent reviews exist describing ILs for analytical chemistry, electroanalytical chemistry or electrochemistry [9, 28–31], here we will focus on the imidazolium-based IL-materials and their applications in electroanalytical chemistry from our laboratory as well as other groups.

## 4.2 ELECTROSYNTHESIS

ILs show a relatively wide potential window and high conductivity and allow studies to be undertaken without additional supporting electrolyte. Recently, Aida et al. have reported sing-walled carbon nanotubes (SWNTs) could be considerably untangled into much finer bundles that are physically cross-linked in ILs [32]. Thus, we were motivated to design a kind of RTIL-supported three-dimensional network SWNT electrode (as shown in [Fig. 4.1a](#)) [33]. The advantage of bucky gels of ionic

liquids and SWNTs for the electrochemical functionalization of SWNTs is that the ionic liquid acts as both a dispersant of SWNTs and a supporting electrolyte. More important, it would greatly increase the effective surface area of the SWNT electrode, and the homogeneous electrochemical functionalization of the SWNTs performed well even in large quantities. This is rare for conventional electrochemical functionalization of SWNTs because the reaction occurs locally on a limited surface of bundled SWNTs deposited on metal electrodes. N-succinimidyl acrylate (NSA), as a model monomer, which bears an active ester group, was ground into a gel of ILs and SWNTs, and the mixture was placed onto gold electrode. NSA was electrografted and polymerized onto SWNTs (SWNTs-poly-NSA) by applying a reduction potential to the electrode (Fig. 4.1b). The active ester groups in the grafted poly-NSA can be utilized for further functionalization. For example, by the reaction with glucose oxidase (GOD), the modified SWNTs with an electrocatalytic activity toward glucose can be fabricated, which could be utilized as biosensor toward glucose (Fig. 4.1c). Similarly, Wei et al. have utilized the same method to functionalize SWNTs with polyaniline [34].

In addition, ILs could also be used as both solvent and electrolyte for the electrodeposition of copper [35, 36], aluminum [37, 38], tantalum [4], platinum [39], silver [40, 41], gold [40–42], and silicon [43]. For example, Endres et al. have reported the electrodeposition of nanocrystalline metals and alloys, such as aluminum from ILs, which previously could not be electrodeposited from aqueous or organic solutions. This method enabled the synthesis of aluminum nanocrystals with average grain sizes of about 10 nm, Al–Mn alloys, as well as Fe and Pd nanocrystals [4] (as shown in Fig. 4.2).

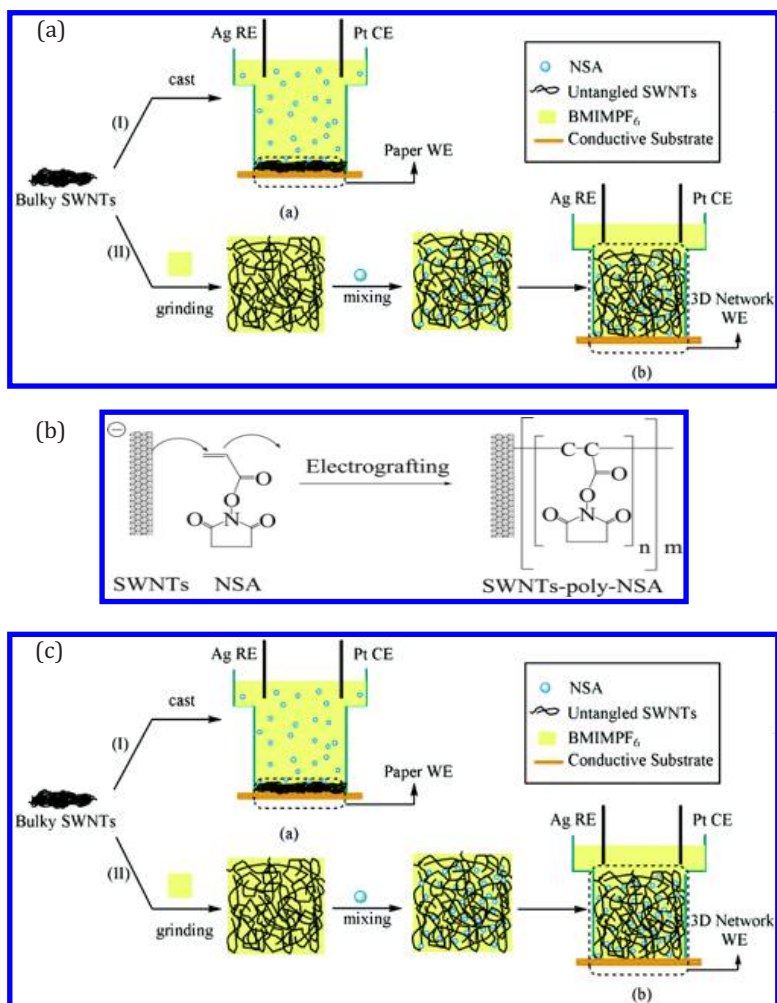


**Figure 4.1** (a) Electrochemical functionalization at the SWNTs paper electrode (I) and our 3D network SWNTs electrode (II). (b) Schematic illustration of grafting NSA on SWNTs via electrochemical initiation and (c) LSV curves of electrocatalyzed oxidation of glucose in 0.05 M PBS (pH 7.4) on the SWNTs-poly-NSA-GOD electrode at different concentrations of glucose: 0, 4, 8, 12, 16, 20 mM from bottom to up. Inset is calibration curve corresponding to amperometric responses at the SWNTs-poly-NSA-GOD (solid) and SWNTs-poly-NSA (hollow) modified gold electrodes. Scan rate: 50 mV/s. Reprinted with permission from Ref. [33]. Copyright 2005 American Chemical Society.

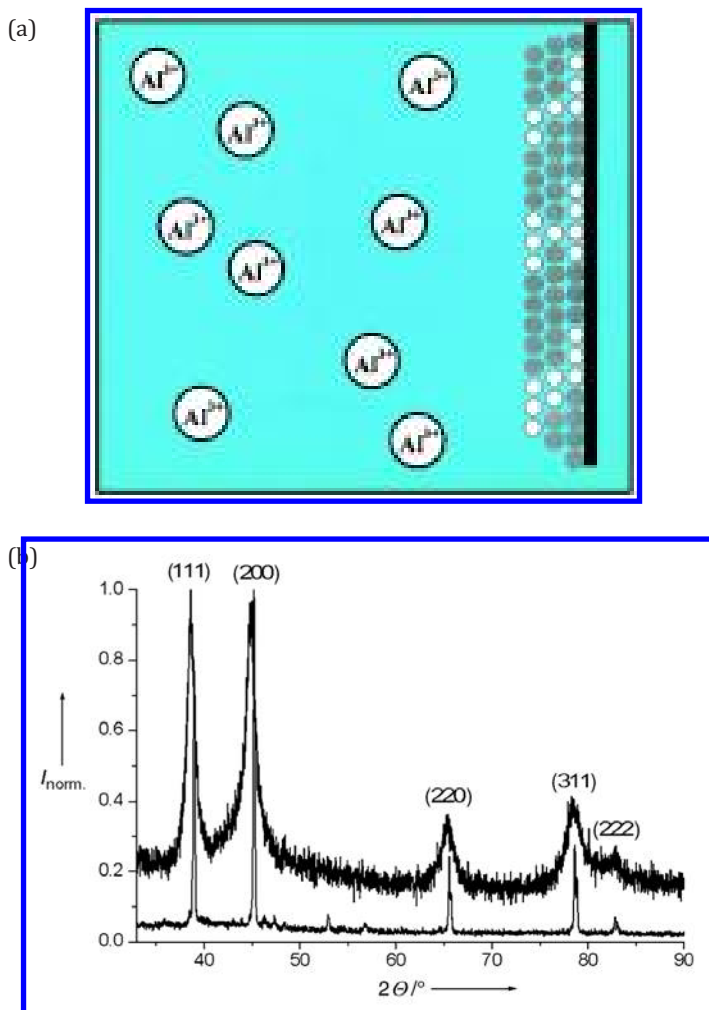
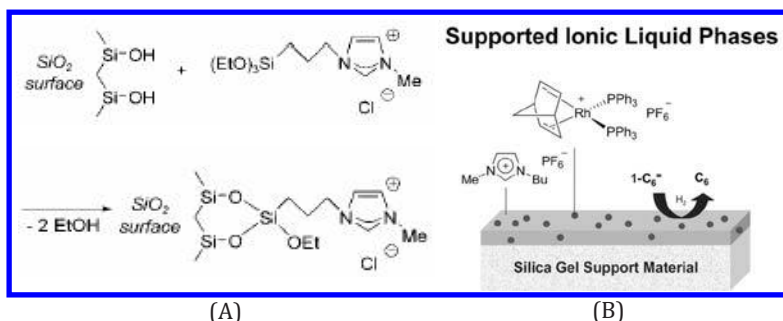


**Figure 4.2** (a) schematic representation of electrodeposition of Al in ILs and (b) Upper curve: XRD pattern of nanocrystalline Al with a grain size of  $12 \pm 1$  nm prepared from  $\text{AlCl}_3/[\text{BMIm}]^+\text{Cl}^-$  (55/45 mol%). Lower curve: Microcrystalline reference sample. From Endres, F., Bukowski, M., Hempelmann, R., and Natter, H. (2003). Electrodeposition of nanocrystalline metals and alloys from ionic liquids. *Angew.Chem. Int. Ed.*, **42**, pp. 3428–3430. Copyright Wiley-VCH Verlag GmbH & Co. KGaA. Reproduced with permission.

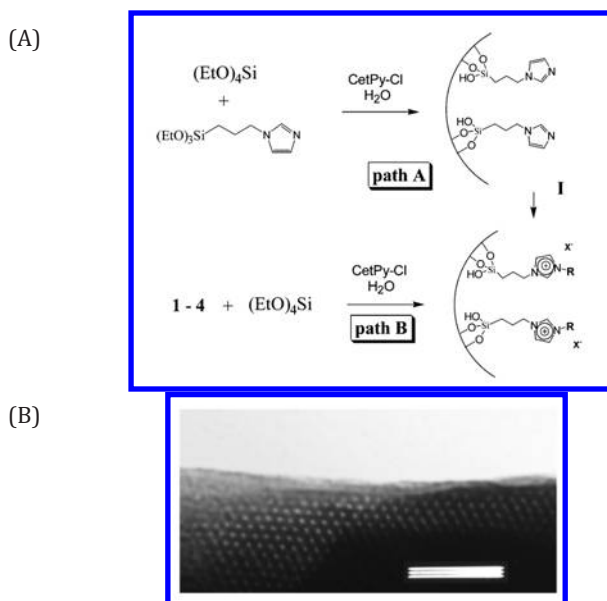
### 4.3 FUNCTIONALIZATION OF IONIC LIQUIDS FOR EASE IMMOBILIZATION

With the development of the synthesis of ILs, the price of ILs has been greatly decreased. However, considering the economic criteria, the ease of separation and increasing the recycle times, the immobilization of ILs on the solid supports is highly desirable. The immobilization process transferred the desired properties of ILs to the solid supports. And more important, to date, difficulties in effective immobilization of generic ILs on the electrode substrate have greatly hindered research on the electrocatalysis of ILs. It was reported that the ILs can be bound to a surface by either covalent bonds or noncovalent interactions between the ILs and the surface. Mehnert et al. have first proposed the concept of silica-supported ILs catalysis, where the ILs immobilized on the Si/SiO<sub>2</sub> surface was functionalized with alkyl siloxane appendages (Fig. 4.3) [24, 44]. Similarly, ionic species were immobilized on the surface of mesoporous nanostructured silicas by Moreau et al. (Fig. 4.4) [45]. Lee and coworkers [46] have proposed a method to immobilize ILs on gold surface, which was based on self-assembly with imidazolium ions bearing alkyl thiol (Fig. 4.5a). Interestingly, simply by anion exchange, the wettability of gold surface could be facily controlled (Fig. 4.5b). Huck et al. developed IL based polyelectrolyte brushes, which were anchored on Au surface via thiol initiator, e.g., BrC-(CH<sub>3</sub>)<sub>2</sub>COO(CH<sub>2</sub>)<sub>6</sub>SH. Further by ion exchange with ferricyanide ions ([Fe(CN)<sub>6</sub>]<sup>3-</sup>) as redox probes, CV measurements of the modified brushes showed the typical electrochemical response corresponding to a surface-confined electroactive species and the redox counterions, as ferricyanide species form stable ion pairs with the quaternary ammonium groups of the brush (Fig. 4.6) [47]. In a noncovalent way, Mao et al. have reported that ILs could be directly immobilized on the glassy carbon electrode (GC) by casting and observed the electrocatalytic activity toward ascorbic acid (AA) and the capability to facilitate direct electron transfer of horseradish peroxidase (HRP) (Fig. 4.7) [48]. Dong et al. have reported

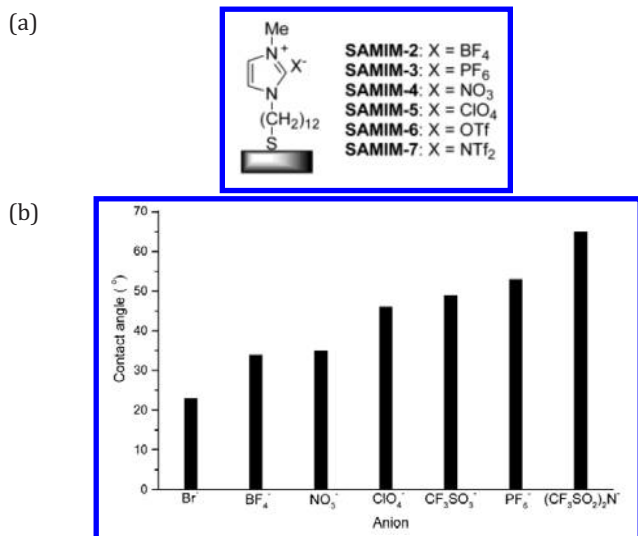
ILs-carbon composites-pastes modified electrode and its efficient electron transfer between the electrode and the horseradish peroxidase (HRP, Fig. 4.8) [49].



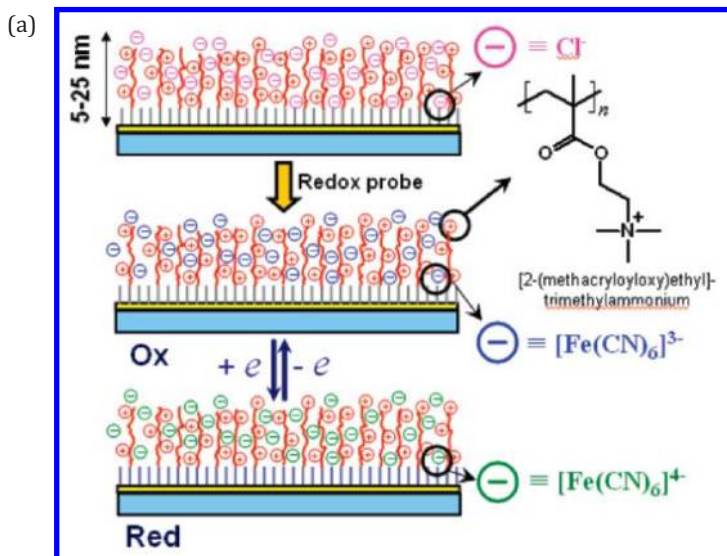
**Figure 4.3** Immobilization of chloroaluminate-based ionic liquid by grafting of imidazolium chloride (A) and the scheme of the concept of supported ILs (B). From Mehnert, C. P. (2005). Supported ionic liquid catalysis. *Chem. Eur. J.*, **11**, pp. 50–56. Copyright Wiley-VCH Verlag GmbH & Co. KGaA. Reproduced with permission.



**Figure 4.4** Schematic (A) and TEM image (B) of Immobilization of ionic species on the surface of mesoporous nanostructured silicas [45]. Reproduced by permission of The Royal Society of Chemistry.



**Figure 4.5** Self-assembled monolayers presenting imidazolium ions at the tail ends on Au having different anions (a) and the effects of counteranions on surface hydrophilicity and hydrophobicity (b). Reprinted with permission from Ref. [46]. Copyright 2004 American Chemical Society.



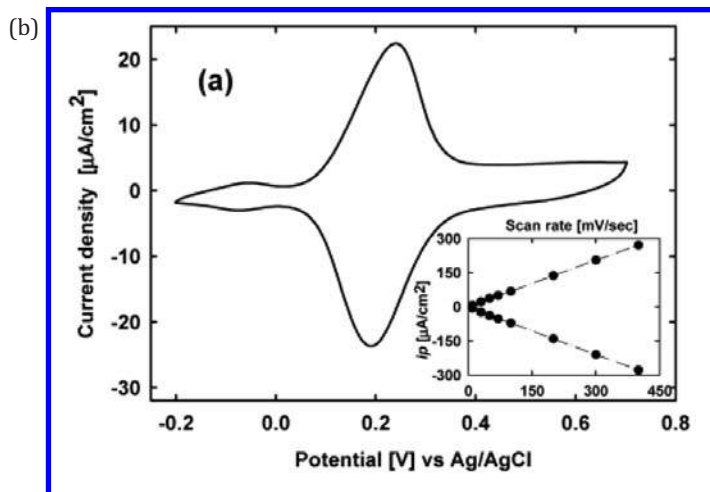


**Figure 4.6** (a) Schematic representation of IL-based polyelectrolytes brushes. (b) Cyclic voltammogram corresponding to electroactive brush (14 nm).  $v$ : 30 mV/s. Supporting electrolyte: 5 mM KCl. Inset: Plot of anodic and cathodic peak currents versus  $v$ . Reprinted with permission from Ref. [47]. Copyright 2007 American Chemical Society.

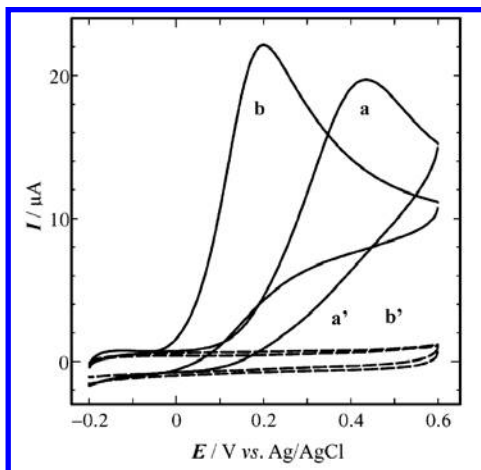


**Figure 4.7** CVs for the oxidation of AA (1.0 mM) at bare (curve a) and 1-butyl-3-methyl imidazolium chloride ([BMIM][Cl])-modified (curve b) GC electrodes in 0.10 M phosphate buffer. Curves a and b represent CVs obtained at the above electrodes in the same solution containing no AA. Scan rate, 100 mV s<sup>-1</sup>. Reprinted with permission from Ref. [48]. Copyright 2005 American Chemical Society.

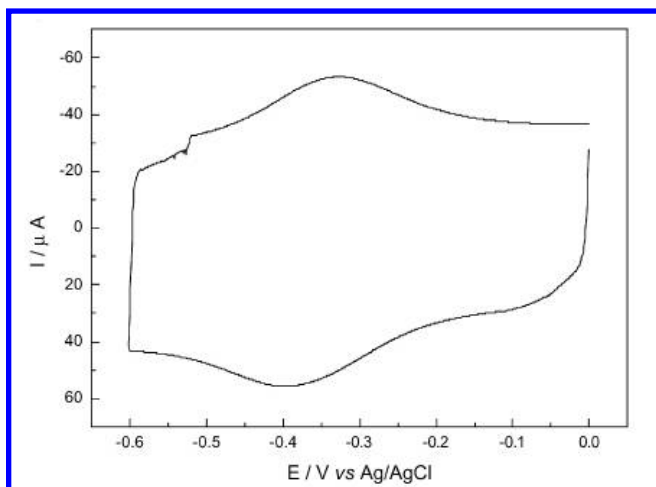


**Figure 4.8** Cyclic voltammogram at the HRP/CNTs/1-butyl-3-methylimidazolium hexafluorophosphate-modified glassy carbon electrode in 0.1 M phosphate buffer solution (pH = 7.00) under nitrogen. The scan rate is 0.1 V/s. Reprinted with permission from Ref. [49]. Copyright 2004 American Chemical Society.

Our strategy for solving above challenge involves preparation of the polyelectrolyte-supported ILs (PFIL, Fig. 4.9) [50] It was noted that polyelectrolyte could be easily immobilized onto many substrates through various methods such as electrophoresis, layer-by-layer (LbL) assembly and casting, etc. Therefore, it would be helpful for us to immobilize ILs facily on general substrates with the aid of polyelectrolyte as carrier. Thus, the ILs could be easily immobilized on the substrate with the aid of polyelectrolyte. As illustrated, the direct electrocatalytic activity of the PFIL toward the oxidation of  $\beta$ -Nicotinamide adenine dinucleotide (NADH) was reported for the first time. In addition, via LbL assembly of PFIL, an electrochemically controlled tunable surface was also constructed. Such design of PFIL provided more general approaches to immobilize IL on any solid supports in spite of any size and shape, and it would be much significant for the chemical industrial processes. This practical advantage of the PFIL material was technically attractive in chemical industrial processes, and exhibited a significant future toward the application of IL wherever in surface chemistry or in catalytic chemistry.

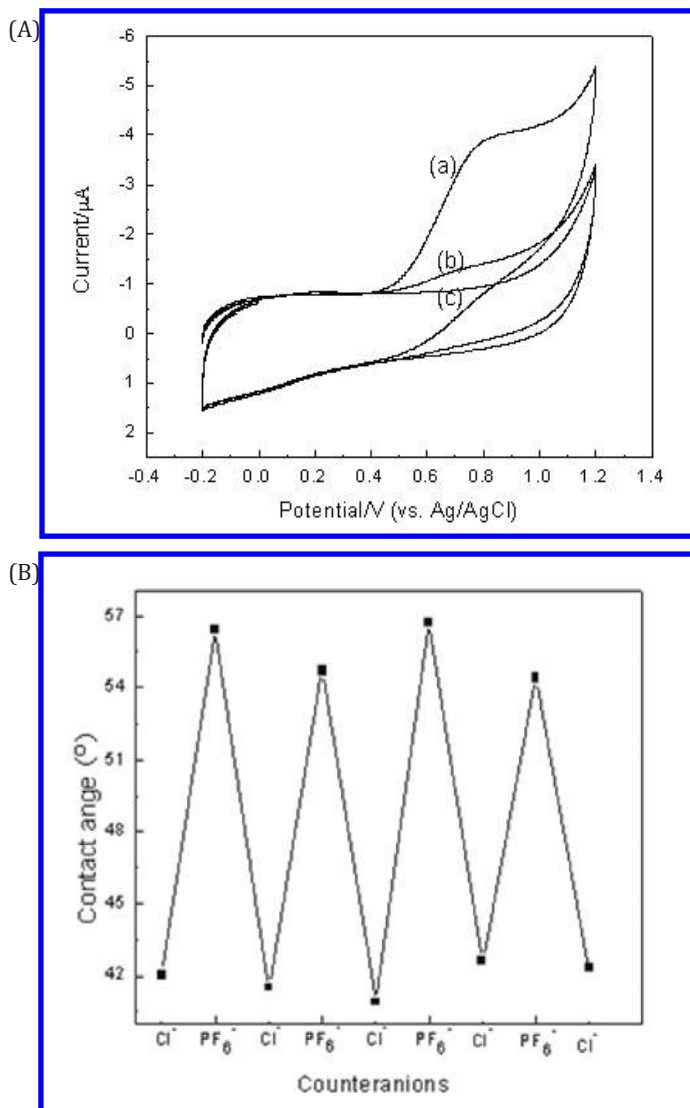


**Figure 4.9** (A) Cyclic voltammograms for 0.5 mM NADH in phosphate buffer solution (0.05 M, pH = 7.4) at PFILs-Nafion (a), Nafion (b) modified GC, and only in phosphate buffer solution (0.05 M, pH = 7.4) at PFIL-Nafion modified GC (c). Inset shows scheme of PFIL. (B) Reversible change in wettability by applying an electric field onto the substrate in 10 mM  $\text{NaPF}_6$  or  $\text{NaCl}$  solution. Working potential: +0.3 V; time scanning: 600 s [50]. Reproduced by permission of The Royal Society of Chemistry.

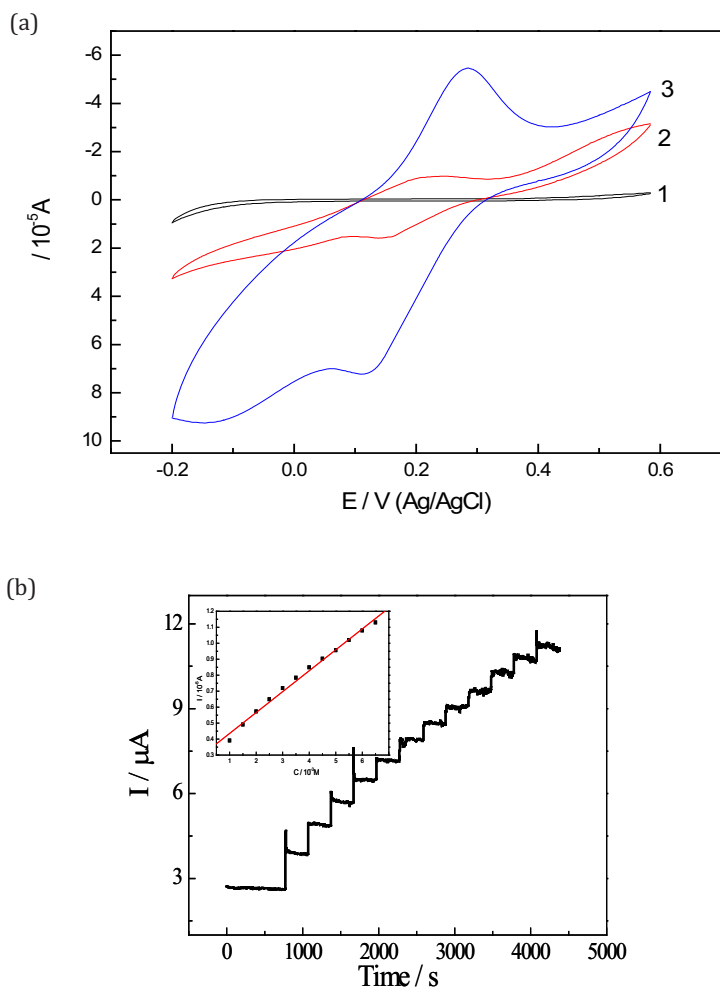


**Figure 4.10** The cyclic voltammograms of the blank ITO electrode (1) ITO/(PDDA/PB)10 multilayer films (2) and ITO/(PFIL/PB)10 multilayer films electrodes (3) in 0.1 M KCl solution saturated with  $N_2$  at the scan rate of 50 mV/s in the present of 0.25 mM  $H_2O_2$  (A); Steady-state response of ITO/(PFIL/PB) 10 electrode with successive addition of 0.25 mM  $H_2O_2$  into stirring 0.1 M KCl solution. (Applied potential:  $-0.1$  V vs. Ag|AgCl in saturated KCl.) Inset: the calibration curve (B) Reproduced with permission from Ref. [51]. Copyright Elsevier (2008).

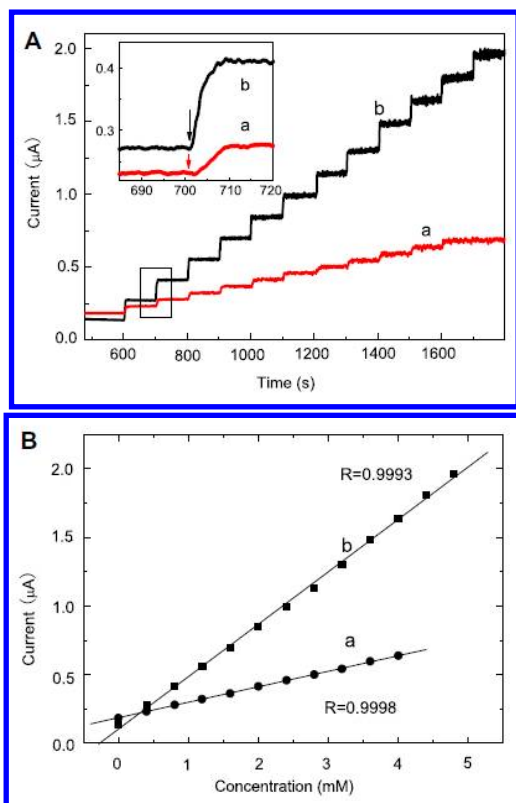


**Figure 4.11** (A) Steady-state response of (a) GOD/sol-gel/GC and (b) GOD/PFIL/sol-gel/GC electrodes with successive addition of glucose concentration (0.4 mmol/L each step). Applied potential: 1.05 V vs. Ag|AgCl (in saturated KCl). Inset shows a magnification of the second addition of glucose. (B) Calibration curves of the above (a), (b) electrodes. Reproduced with permission from Ref. [52]. Copyright Elsevier (2007).

From another point of view, polyelectrolyte functionalized IL was also a novel kind of polyelectrolyte. Thus, many traditional applications of polyelectrolytes would be possible for such PFIL and some unique properties derived from ILs would also be expected. For example, ultrathin films of PFIL and Prussian blue (PB) nanoparticles were fabricated on the ITO substrate through electrostatic layer-by-layer assembly method [51]. The obtained PFIL/PB multilayer showed good reproducibility, wide linear

range, and high sensitivity (even to  $10^{-7}$  M) for the amperometric analysis of hydrogen peroxide, which was superior to a similar Poly (diallyldimethyldiammonium chloride) (PDDA)/PB multilayer in the control experiments (Fig. 4.10). It indicated that the PFIL on the modified electrode played an important role in the electrocatalytic reduction of hydrogen peroxide.

Similarly, polyelectrolytes functionalized IL could be incorporated into a sol-gel organic-inorganic hybrid material (PFIL/sol-gel) to improve charge-transfer efficiency and substrate diffusion in chemically modified electrodes [52]. By immobilizing GOD on a glassy carbon electrode, an enhanced current response toward glucose was obtained, relative to a control case without PFIL. In addition, chronoamperometry showed that electroactive mediators diffused at a rate 10 times higher in the apparent diffusion coefficient in PFIL-containing matrices (Fig. 4.11). These findings suggest a potential application in bioelectroanalytical chemistry.

#### 4.4 ELECTROLYTE-FREE ELECTROCHEMISTRY

It is common practice that electrochemical experiments should be conducted in the presence of supporting electrolytes. However, within last few years, the general necessity to add an excess of supporting electrolyte has been questioned, and it is desirable to consider even the necessity of using a supporting electrolyte in various cases. Some promising methods for electrolyte-free electrochemistry such as with ultramicroelectrodes (UMEs) or their modifications with moist ion-exchange membranes such as Nafion have been developed. We have reported an alternative pathway by a simple PFIL-modified electrode (Fig. 4.12) [53]. The studied PFIL material combines features of ionic liquids and traditional polyelectrolytes. The IL part provides high ionic conductivity and affinity to many different compounds. The polyelectrolyte part has a good stability in aqueous solution and capability to be immobilized on different substrates. The electrochemical properties of such a PFIL-modified electrode assembly in supporting electrolyte-free solution have been investigated by using an electrically neutral electroactive species, hydroquinone (HQ) as the model compound.

The partition coefficient and diffusion coefficient of HQ in the PFIL film were calculated to be 0.346 and  $4.74 \times 10^{-6} \text{ cm}^2 \text{ s}^{-1}$ , respectively. Electrochemistry in PFIL is similar to electrochemistry in a solution of traditional supporting electrolytes in the solution, except that the electrochemical reaction takes place in a thin film on the surface of the electrode. PFIL is easy to be immobilized on solid substrates, inexpensive and electrochemically stable. A PFIL-modified electrode assembly is successfully used in flow analysis at HQ by amperometric detection in solution without supporting electrolyte. Similarly, polypyrrole could be electropolymerized on PFIL-PSS modified electrodes without added support electrolytes [54].

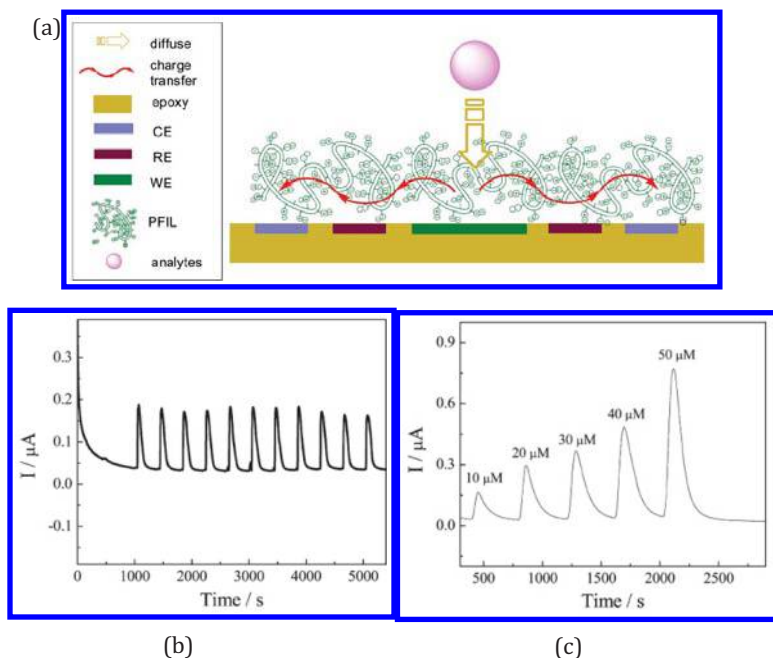


**Figure 4.12** Illustration of the electrochemical process of the analytes at the PFIL-modified electrode assembly in a supporting electrolyte-free solution (a); amperometric responses of repeated injection of a 20  $\mu\text{M}$  HQ solution (b); amperometric response of HQ at different concentrations. The signal was recorded at the 1.4 mm-thick PFIL-modified electrode assembly at +0.3 V. Double-distilled water was used as the carrier solution. Flow rate: 1  $\text{mL min}^{-1}$  (c) [53]. Reproduced by permission of The Royal Society of Chemistry.

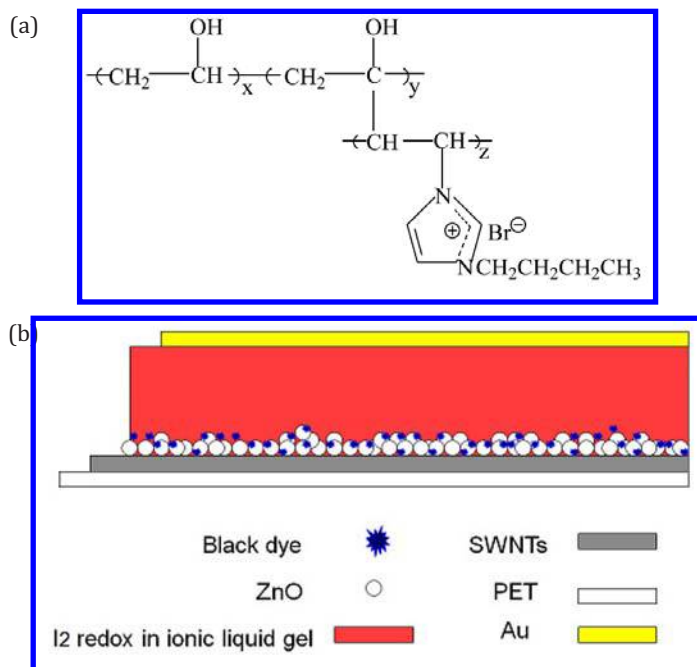


**Figure 4.13** Structure of (a) PVA-g-VIC4Br and (b) solid-state DSSC. Reproduced with permission from Wei, D., Unalan, H. E., Han, D. X., Zhang, Q. X., Niu, L., Amaratunga, G., and Ryhanen, T. (2008). A solid-state dye-sensitized solar cell based on a novel ionic liquid gel and ZnO nanoparticles on a flexible polymer substrate. *Nanotechnology*, **19**, pp. 424006–424010.

Actually, PFIL on the electrode assembly offered a suitable electrochemical microenvironment for electrochemical reaction; in this case, it was not absolutely electrolyte free. Thus, it also hints functionalized IL could be used as solid-state electrolyte for some specific applications, such as solar cells. Figure 4.13b shows a full solid-state, flexible, dye-sensitized solar cell (DSSC) based on novel ionic liquid gel (PVA-g-VIC4Br), organic dye, ZnO nanoparticles, and CNTs thin film stamped onto a polyethylene terephthalate (PET) substrate [55]. It would pave the way for the development of a continuous roll-to-roll process for the mass production of flexible and lightweight DSSCs.

## 4.5 ILS-BASED MULTIFUNCTIONAL COMPOUNDS FOR ELECTROCATALYSIS AND BIOSENSORS

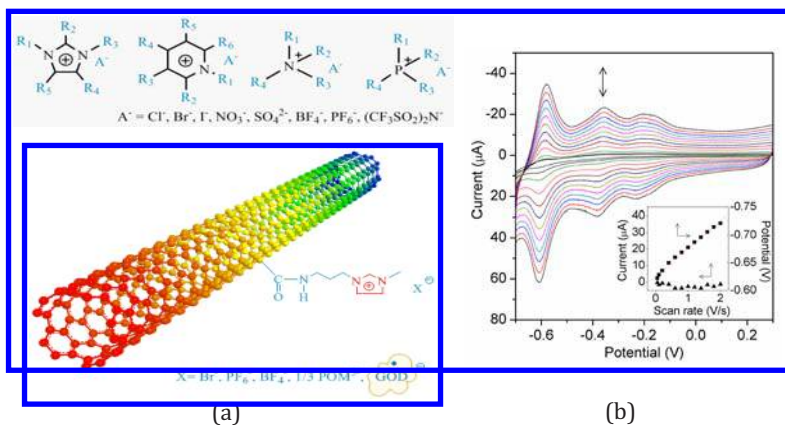


**Figure 4.14** (a) Examples of cations and anions commonly used for the formation of ionic liquids and SWNT-IL-X. (b) Cyclic voltammograms (CVs) of SWNT-IL-POM modified GC electrode ( $d = 3$  mm) at different scan rate in 0.5 M  $\text{H}_2\text{SO}_4$ . Scan rate: 0.05, 0.1, 0.2, 0.4, 0.6, 0.8, 1.0, 1.2, 1.4, 1.6, 1.8 and 2.0 V/s from inner to outer. The inset shows the peak current (square) and peak potential (triangle) of the third reduction wave as a function of scan rate. From Zhang, Y. J., Shen, Y. F., Yuan, J. H., Han, D. X., Wang, Z. J., Zhang, Q. X., and Niu, L. (2006). Design and synthesis of multifunctional materials based on an ionic-liquid backbone. *Angew. Chem. Int. Edit.*, **45**, pp. 5867–5870. Copyright Wiley-VCH Verlag GmbH & Co. KGaA. Reproduced with permission.

One of the most fantastic features of ILs is that their properties can be easily and well tuned by rationally selecting proper combination of organic cations and anions. That also means that we can delicately utilize one ionic component to deliver a unique function and the other ionic component to deliver a different, completely independent function. Moreover, the components and their combination of anions and cations are various, for example, the cation of ILs can have several substituting groups (R1, R2, R3, etc., as shown in Fig. 4.14a) and these substituting groups are tunable. Therefore, it offers us a promising and facile way to combine individual functions into a target compound. In contrast, for a commonly seen compound, to achieve this multifunctional combination would encounter all

sorts of synthetic challenges. We have illustrated this flexibility of ILs by selecting SWNT (R1) as a model substituting group of the imidazolium cation, and  $\text{Br}^-$ ,  $\text{PF}_6^-$ ,  $\text{BF}_4^-$ , polyoxometalates (POMs), and even glucose oxidase (GOD) as the counter-anions (Fig. 4.14a, SWNT-IL-X) [56]. The properties of SWNT and the various anions were facilely and successfully delivered into the resulting compounds. For example, the rich redox activity was also successfully transferred into SWNT-IL-POM merely by a simple and facile anions exchange. The surface-confined SWNT-IL-POM shows three couples of well-defined redox waves at scan rates up to 2 V/s (Fig. 4.14b), which was presumably attributed from electron conduction of SWNT, ionic conduction of IL, and redox conduction of POM. It was unusual for an often-seen compound in electrochemical systems.

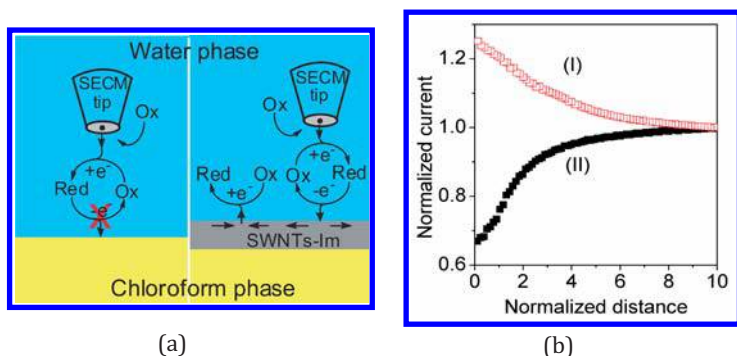
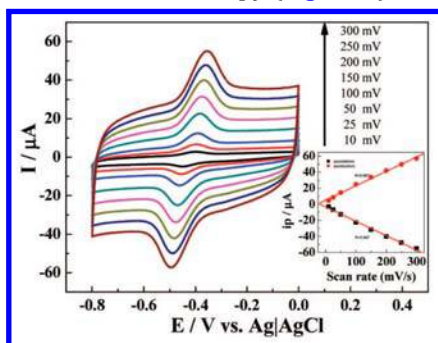


**Figure 4.15** (a) SECM arrangement (not to scale) for feedback measurement at pure (left) and SWNTs-Im-sandwiched (right) water/chloroform interface; (b) Experimental approach curves (CHI 900) for a tip in aqueous solution approaching SWNTs-Im-sandwiched (I) and pure (II) water/chloroform interface. Currents are normalized to the steady-state diffusion limiting current,  $i_{T,\infty}$  and distance to tip radius. The aqueous solution contained 0.5 mM  $\text{Ru}(\text{NH}_3)_6^{3+}$  and 100 mM KCl. The tip (Pt, 10  $\mu\text{m}$  radius, RG = 10) was held at  $-0.35$  V vs. Ag|AgCl (saturated KCl) for  $\text{Ru}(\text{NH}_3)_6^{3+}$  reduction and approached at 1  $\mu\text{m/s}$ . The counter electrode was Pt wire [58]. Reproduced by permission of The Royal Society of Chemistry.

Moreover, due to the controllable wettability by counter-anion exchange [56, 57], SWNT-IL-Br, which was both hydrophobic and hydrophilic, could assemble at the water/oil interface in a controllable manner, i.e., from monolayer to multilayers [58]. Thus, it enabled a novel SWNT-sandwiched water/oil interface for the

electron transfer, one of the most fundamental chemical processes across the interfaces. It will promote both fundamental electron transfer research such as in biological and artificial membrane and homo/heterogeneous catalysis. For example, it indicated SWNTs accelerated the electron transfer at water/oil interface by using scanning electrochemical microscopy (Fig. 4.15).

(a)



(b)

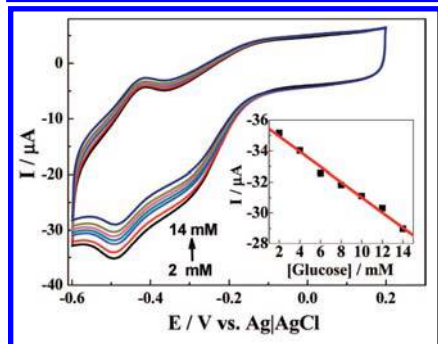


**Figure 4.16** Cyclic voltammetric measurements at GCE/graphene-IL-GOD electrode in 0.05 M N<sub>2</sub> saturated PBS solution at different scan rates. Scan rate: 0.02, 0.05, 0.1, 0.15, 0.2 V s<sup>-1</sup> from inner to outer. Inserted is the calibrated plot of peak currents versus scan rates (a) (reprinted from *Biosens. Bioelectron.*, **23**, Zhang, Y., Shen, Y., Han, D., Wang, Z., Song, J., Li, F., and Niu, L., Carbon nanotubes and glucose oxidase bionanocomposite bridged by ionic liquid-like unit: Preparation and electrochemical properties, 438–443, copyright 2007, with permission from Elsevier). Cyclic voltammetric curves at the GCE/graphene-IL-GOD electrode in various concentrations (2, 4, 6, 8, 10, 12, and 14 mM) of glucose PBS solution saturated with O<sub>2</sub>. The inset is the calibration curve ( $R=0.994$ ) corresponding to amperometric responses at  $-0.49$  V. Scan rate: 0.05 V s<sup>-1</sup> (b) (reprinted with permission from Ref. [60], copyright 2009 American Chemical Society).

For its potential bioelectroanalytical and biomedical application, integration of carbon nanostructures such as CNTs and graphene nanosheets with biomolecules such as redox enzyme is highly anticipated. Therein, carbon nanostructures are expected to act not only as an electron transfer promoter or mediator, but also as substrates for biomolecules immobilization. Based on ionic liquid-backbone, a novel immobilization method for biomolecules on carbon nanostructures could also be achieved via ionic interaction, which is of universality and widespread use in biological system. As illustrated, glucose oxidase (GOD) and SWNTs and graphene nanosheets were integrated into one bionanocomposite with the aid of ionic liquid-like unit on functionalized SWNTs [59] or PFIL wrapped Polyvinylpyrrolidone (PPV)-graphene [60]. Results indicated that the ionic liquid-like unit on SWNTs, which did not depend on pH, would provide an extra and stronger ionic affinity between SWNTs and GOD so as to enhance the loading efficiency of GOD on SWNTs (Fig. 4.16). The direct electrochemistry of GOD was also achieved on PFIL wrapped Polyvinylpyrrolidone (PVP)-graphene (Fig. 4.16a). Moreover, in these novel graphene-bionanocomposites, the specific substrate-enzyme bioactivity of GOD in the bionanocomposites was reserved, which could be utilized to build the electrochemical biosensor toward detection of glucose (Fig. 4.16b).



**Figure 4.17** Illustration of the preparation procedures of CNT-IL-Au Reprinted from Carbon, 46, Wang, Z., Zhang, Q., Kuehner, D., Xu, X., Ivaska, A., and Niu, L., The synthesis of ionic-liquid-functionalized multiwalled carbon nanotubes decorated with highly dispersed Au nanoparticles and their use in oxygen reduction by electrocatalysis, 1687–1692, copyright 2008, with permission from Elsevier.

Similarly, nanoparticles (NPs) could also be integrated in to nanocomposites based on the ILS-backbone. The approach involved the functionalization of CNTs with amine-terminated ILS and in

situ reduction of  $\text{HAuCl}_4$  without any additional step to introduce other reducing agents (Fig. 4.17) [61]. This composite material showed good electrocatalytic activity toward reduction of oxygen. In addition, the results of control experiments confirmed that the presence of ILs and the small size of gold nanoparticles increase the electrocatalytic activity of CNTs greatly.

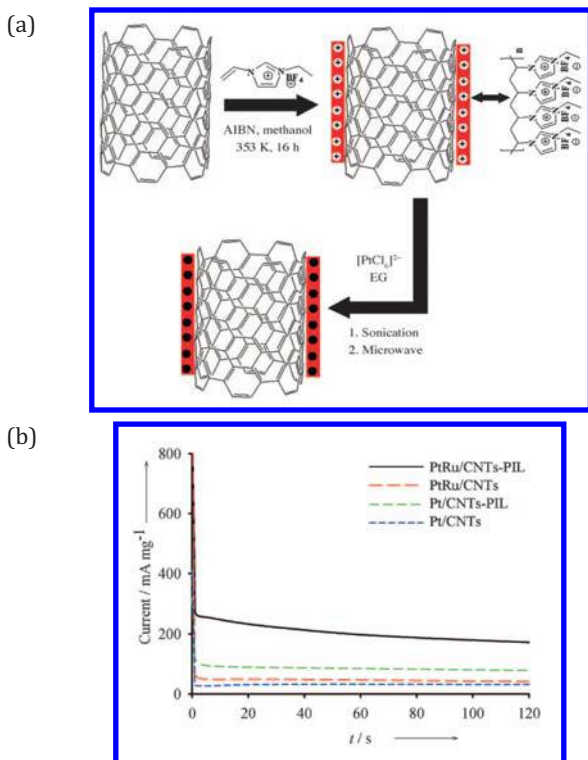


**Figure 4.18** (a) Schematic diagram of the modification of CNTs with PIL and the preparation of Pt/CNTs-PIL nanohybrids. EG: ethylene glycol, AIBN: 2,2'-azobisisobutyronitrile. (b) Transient current of PtRu/CNTs-PIL, PtRu/CNTs, Pt/CNTs-PIL, and Pt/CNTs catalysts for methanol electrooxidation at 0.50 V in nitrogen-saturated 0.5 M  $\text{H}_2\text{SO}_4$  + 1.0 M  $\text{CH}_3\text{OH}$  aqueous solution. From Wu, B. H., Hu, D., Kuang, Y. J., Liu, B., Zhang, X. H., and Chen, J. H. (2009). Functionalization of carbon nanotubes by an ionic-liquid polymer: dispersion of Pt and PtRu nanoparticles on carbon nanotubes and their electrocatalytic oxidation of methanol. *Angew. Chem. Int. Edit.*, **48**, pp. 4751–4754. Copyright Wiley-VCH Verlag GmbH & Co. KGaA. Reproduced with permission.

Besides, ILs unit could be attached to the sidewall of CNTs by radical grafting, in which acid-oxidation pretreatment of CNTs could be avoided. Chen et al. reported that thermal-initiation free radical polymerization of the IL monomer 3-ethyl-1-vinylimidazolium tetrafluoroborate ( $[\text{VEIM}]\text{BF}_4$ ) on the CNT surface (Fig. 4.18a) [62]. Then under similar method, the Pt and PtRu nanoparticles with narrow size distribution (average diameter:  $(1.3 \pm 0.4)$  nm for PtRu,  $(1.9 \pm 0.5)$  nm for Pt) are dispersed uniformly on the CNTs and show better performance in methanol electrooxidation than that without ILs units (Fig. 4.18b).

#### 4.6 ILS-PROTECTED NANOSTRUCTURES AS ELECTROCATALYSTS FOR SOME KEY REACTIONS

It was noted that without CNTs, very small Au NPs with an average diameter 1.7 nm could be obtained, where the Au NPs were presumably stabilized by amine-terminated ILs (Fig. 4.19a) [63]. They could be kept stable without any special protection and showed much better electrocatalysis toward reduction of dioxygen (ORR) comparing with those stabilized by thiol or citrate (Fig. 4.19b, c). Moreover, by further immobilizing IL-protected Au NPs on carbon nanostructures, e.g., carbon nanotubes or graphene nanosheets, by static interactions, the ORR current increased up to 6 times, in which the unique electronic property of carbon nanostructures as well as their large active surface areas were believed to play key roles [64, 65]. Here, not only Au NPs but also other noble metal NPs, such as Pt [66], and even graphene nanosheets themselves (Fig. 4.20) [67] could be stabilized by amine-terminated IL, and high electrocatalytic activity toward ORR and oxidation of methanol was also observed.

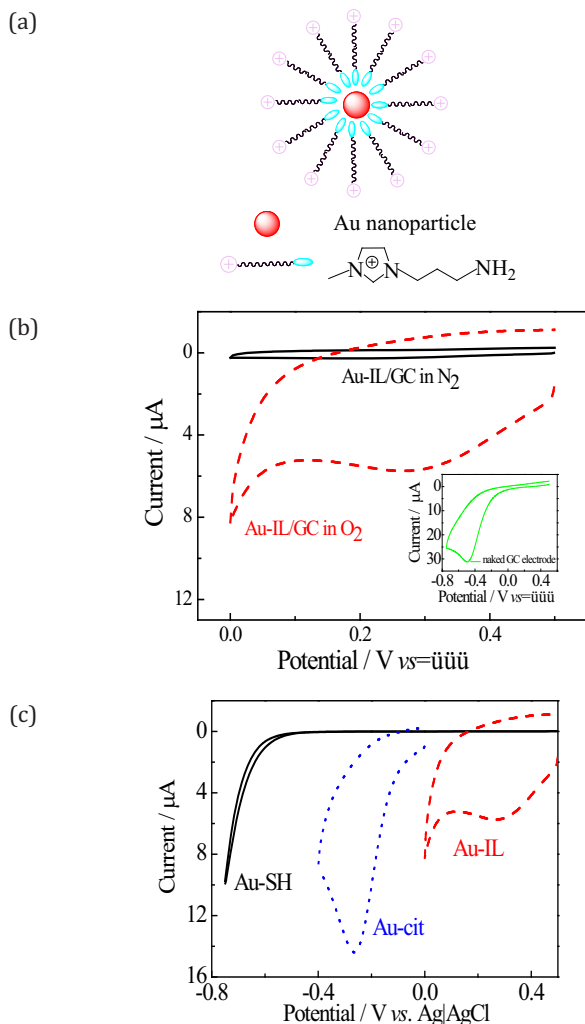


**Figure 4.19** (a) Structure illustration of the resulting Au-IL nanoparticles. (b) Cyclic voltammograms of Au-IL nanoparticles modified GC electrode in 0.5 M  $\text{H}_2\text{SO}_4$  solution saturated with  $\text{O}_2$  (dashed) and  $\text{N}_2$  (solid), respectively. Inset is bare GC electrode in 0.5 M  $\text{H}_2\text{SO}_4$  solution saturated with  $\text{O}_2$ . (c) Cyclic voltammograms of Au-IL nanoparticles (dashed), Au-cit nanoparticles (dotted), and Au-SH nanoparticles (solid) modified GC electrodes in 0.5 M  $\text{H}_2\text{SO}_4$  solution, respectively. Scan rate:  $0.05 \text{ V s}^{-1}$  [63]. Reproduced by permission of The Royal Society of Chemistry.

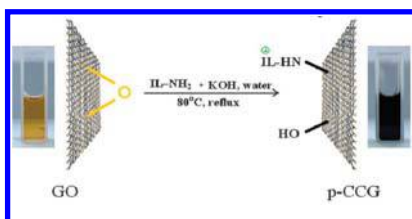


**Figure 4.20** Illustration of the preparation of polydisperse chemically converted graphene (p-CCG) from graphite oxide (GO) by amine-terminated IL [67]. Reproduced by permission of The Royal Society of Chemistry.

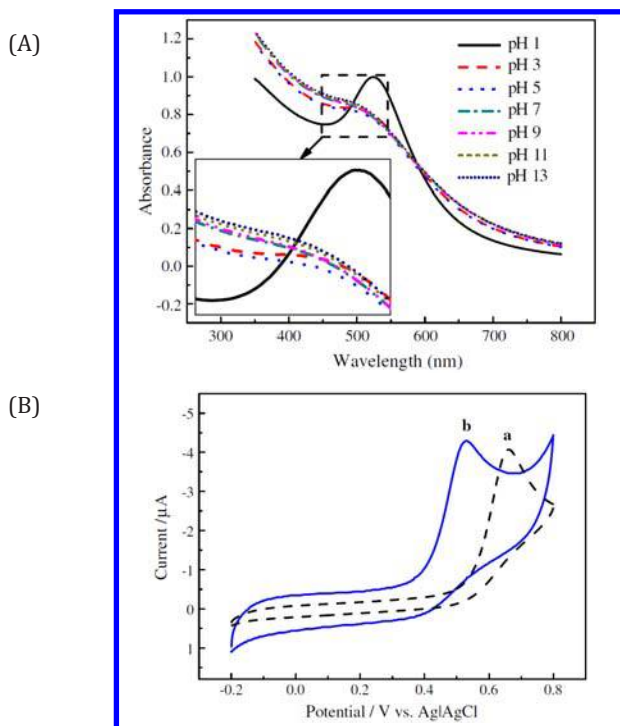


**Figure 4.21** (A) Stability of PFIL-AuNPs in different pH solutions after 2 days storage. The inset shows an enlarged view of the rectangular region. (B) Cyclic voltammograms for 0.5 mM NADH in phosphate buffer solution (0.05 M, pH 7.4) at (a) PFIL, (b) PFIL-AuNP-modified GCE at a scan rate of 0.05 V/s. Reproduced with permission from Shan, C. S., Li, F. H., Yuan, F. Y., Yang, G. F., Niu, L., and Zhang, Q. (2008). Size-controlled synthesis of mono-dispersed gold nanoparticles stabilized by polyelectrolyte-functionalized ionic liquid. *Nanotechnology*, **19**, pp. 285601–285606.

Besides, polyelectrolyte-functionalized IL (PFIL) also showed great potential in stabilization of Au NPs [68]. It was found that the size distribution of resulting Au NPs (PFIL-AuNPs) was narrow and could be tuned by the concentration of  $\text{HAuCl}_4$ . Moreover, they showed a high stability in water at room temperature for at least one month in solutions of pH 7–13 (even in the present of high concentration of NaCl). In addition, the PFIL-AuNPs exhibited obvious electrocatalytic activity toward NADH oxidation, suggesting a potential application for bioelectroanalysis (Fig. 4.21). By further cooperating with electric conductive CNTs, the resulting nanocomposites (CNT-AuNPs-PFIL) showed obvious electrocatalysis toward reduction of  $\text{H}_2\text{O}_2$  and  $\text{O}_2$ . In addition, when glucose oxidase was immobilized into CNT-AuNPs-PFIL thin films, it demonstrated favorable linear catalytic response to glucose [69].

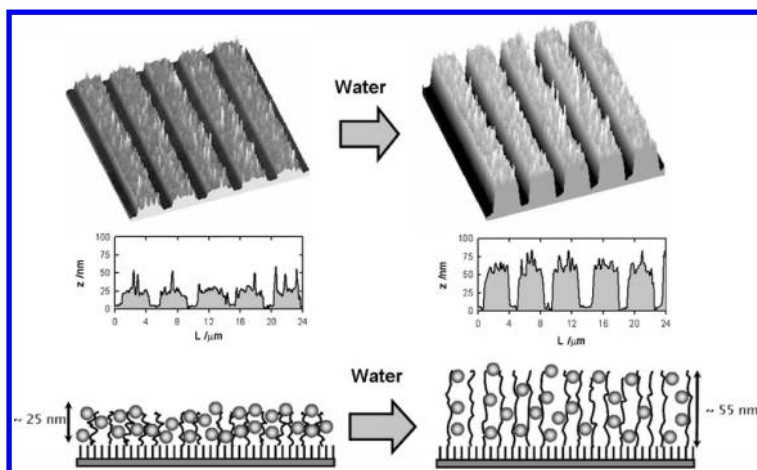


**Figure 4.22** Patterned IL-based polyelectrolytes brushes loaded with AuNPs, in compressed and swollen states (left and right, respectively). Top, middle: AFM images and cross-sectional analyses of patterned brush layers, obtained in air and water; bottom: schematic corresponding to AFM data [70]. Reproduced by permission of The Royal Society of Chemistry.

Huck et al. prepared Au NPs inside IL-based polyelectrolytes [70]. The nanocomposite synthesis relies on loading the macromolecular film with  $\text{AuCl}_4^-$  precursor ions followed by their in situ reduction to Au nanoparticles. It was observed that the nanoparticles are uniform in size and are fully stabilized by the surrounding

polyelectrolyte chains. Moreover, XRR analysis revealed that the Au NPs are formed within the polymer-brush layer. Interestingly, AFM experiments confirmed that the swelling behavior of the brush layer is not perturbed by the presence of the loaded NPs (Fig. 4.22). The Au NP-poly-METAC nanocomposite is remarkably stable to aqueous environments, suggesting the feasibility of using this kind of nanocomposite systems as robust and reliable stimuli-responsive platforms.

## 4.7 OTHERS

Counterions of ILs could be facilely exchanged in solution, thus based on a surfactant with an imidazolium unit, the ion-exchange reaction from bromine ion to hexafluorophosphate ion resulted in the amphiphilic-to-hydrophobic transition of the imidazolium salt, leading to the destruction of the micelles (Fig. 4.23), i.e., an ion-responsive micelle system was proposed [71]. This simple process was rapid, taking only one or two seconds from addition of the hexafluorophosphate ions to precipitation being formed. Furthermore, this procedure was much quicker than dissolution of micelles in response to other external stimuli such as light, heat or pH. Potential application for transportation of oil was highly anticipated, which is easier to pump through pipelines in an emulsified state that is less viscous than oil alone. However, the oil must be easily recoverable from this emulsified state after transportation. Here the ILs surfactant approach satisfied these criteria. Moreover, these smart surfactants would find other applications in the fields of nanoscience and polymer science, which would greatly benefit both fundamental research and industry.

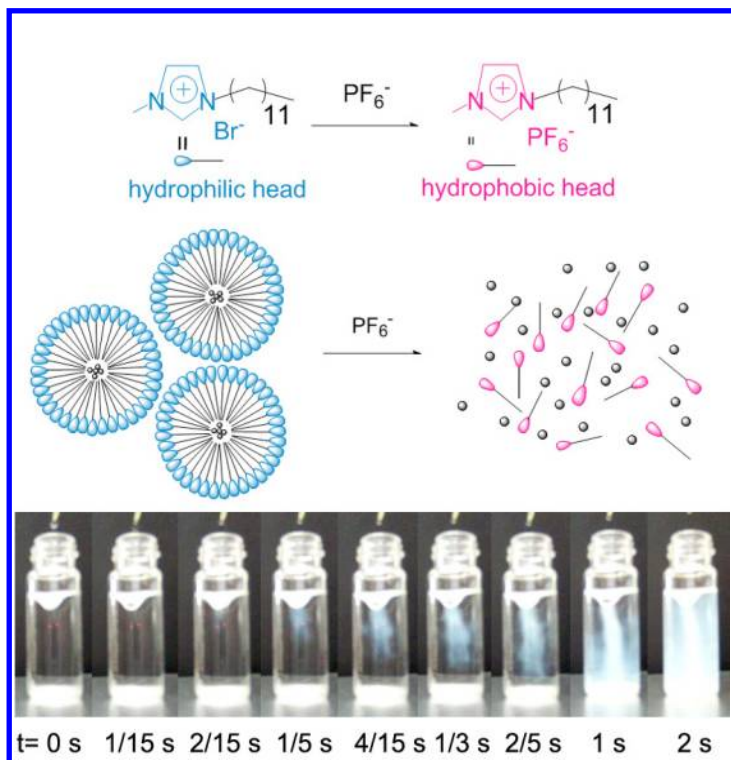


**Figure 4.23** Anion exchange to  $\text{PF}_6^-$  and resulting micelle collapse (above panel), and high-speed photographs showing micelle precipitation after  $12 \mu\text{L}$  of  $3.75\text{M}$   $\text{NaPF}_6$  was pipetted into  $15 \text{ mL}$  of  $10 \text{ mM}$  aqueous  $\text{C}_{12}\text{MIMBr}$  solution ( $0.3$  equiv relative to  $\text{C}_{12}\text{MIMBr}$ ) with mild agitation (bottom panel). From Shen, Y. F., Zhang, Y. J., Kuehner, D., Yang, G. F., Yuan, F. Y., and Niu, L. (2008). Ion-responsive behavior of ionic-liquid surfactant aggregates with applications in controlled release and emulsification. *Chemphyschem*, **9**, pp. 2198–2202. Copyright Wiley-VCH Verlag GmbH & Co. KGaA. Reproduced with permission.

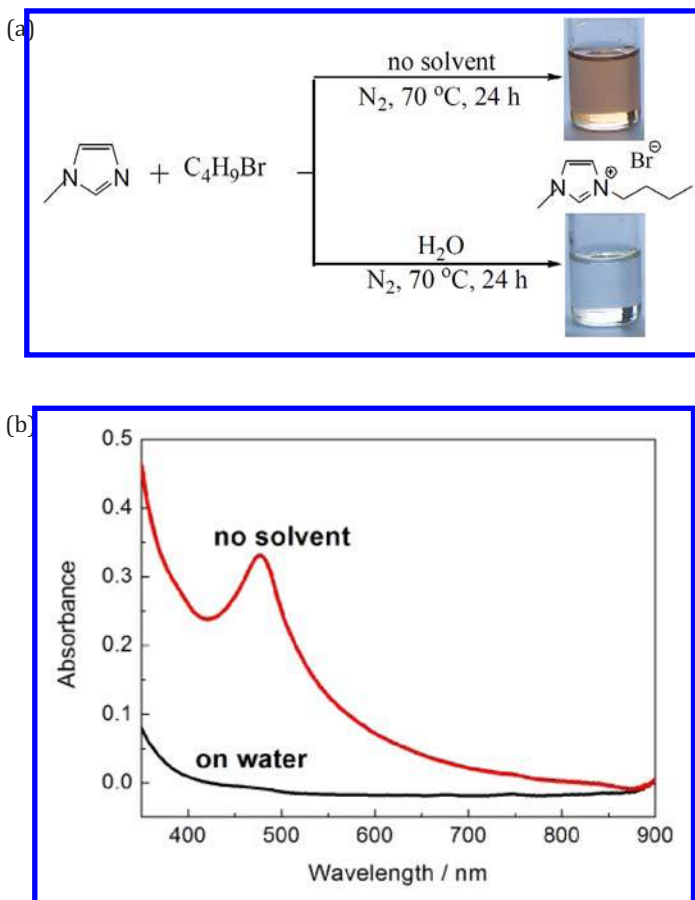


**Figure 4.24** Photographs (a) and UV-Vis absorption spectra (b) of BMIMBr in liquid prepared on water (lower) and without any solvent (upper). Reprinted from *Talanta*, **46**, Shen, Y., Zhang, Y., Han, D., Wang, Z., Kuehner, D., and Niu, L., Preparation of colorless ionic liquids “on water” for spectroscopy, 805–808, copyright 2009, with permission from Elsevier.

Although colorless ILs are most desirable, as prepared ILs frequently bear color, despite appearing pure by most analytical techniques, except for UV-vis spectrum. Thus, it leads to some uncertainties and limits for the fundamental research and

applications of ILs, which has been a longstanding challenge in the field. Using 1-butyl-3-methylimidazolium bromide (BMIMBr), 1-butyl-3-methylimidazolium tetrafluoroborate (BMIMBF<sub>4</sub>) and 1-hexyl-3-methylimidazolium bromide (HMIMBr) as examples, it was demonstrated that following traditional synthesizing method except that the water was added as solvent, colorless ILs could be facily obtained (Fig. 4.24) [72]. In this case, neither critical pretreatment of starting materials and precautions during the reaction nor time-consuming and costly post-decolor-purification was needed. It was believed that in the presence of water, the reactants were biphasic; thus local hot spots due to the higher concentration could be effectively eliminated, which directly produce colorless ILs. It will not only pave the way for economical synthesis of a broad variety of colorless ILs for spectroscopy so as to eliminate the uncertainties and limits but also motivate theoretical and experimental studies to deepen fundamental understanding of the source(s) of color in ILs and enrich the applications of ILs in spectroscopic analytic researches and applications.

## 4.8 CONCLUSIONS

Owing to high ionic conductivity and wide electrochemical window, ILs have the intrinsic advantages for potential applications in electroanalytical chemistry. IL functional materials extend their scope of applications in traditional electroanalytical chemistry merely as green solvents and enable them to be modified on the electrode more conveniently and effectively. Moreover, many other advanced functional compounds could be integrated into multifunctional materials in which ILs act as the backbone. The unique properties of ILs have been well transferred into these ILs materials, and due to synergistic effect, some new electrocatalytic activities are observed. These features enable ILs materials to be promising materials for electroanalytical chemistry. Besides, the concept illustrated here can also be applied to ILs applications in other fields.

## References

1. Wasserscheid, P., and Welton, T. (2002). *Ionic Liquids in Synthesis*; Wiley-VCH: Weinheim.
2. Li, J. H., Shen, Y. F., Zhang, Y. J., and Liu, Y. (2005). Room-temperature ionic liquids as media to enhance the electrochemical stability of self-assembled monolayers of alkanethiols on gold electrodes. *Chem. Commun.*, pp. 360–362.
3. Choi, D. S., Kim, D. H., Shin, U. S., Deshmukh, R. R., Lee, S. G., and Song, C. E. (2007). The dramatic acceleration effect of imidazolium ionic liquids on electron transfer reactions. *Chem. Commun.*, pp. 3467–3469.
4. Endres, F., Bukowski, M., Hempelmann, R., and Natter, H. (2003). Electrodeposition of nanocrystalline metals and alloys from ionic liquids. *Angew.Chem. Int. Ed.*, **42**, pp. 3428–3430.
5. Dobbs, W., Suisse, J.-M., Douce, L., and Welter, R. (2006). Electrodeposition of silver particles and gold nanoparticles from ionic liquid-crystal precursors. *Angew. Chem. Int. Ed.*, **45**, pp. 4179–4182.
6. Ohno, H. (2005) *Electrochemical Aspects of Ionic Liquids*; John Wiley & Sons: Hoboken, New Jersey.
7. Fukushima, T., and Aida, T. (2007). Ionic liquids for soft functional materials with carbon nanotubes. *Chem. Eur. J.*, **13**, pp. 5048–5058.
8. Abbott, A. P., Capper, G., McKenzie, K. J., and Ryder, K. S. (2007). Electrodeposition of zinc-tin alloys from deep eutectic solvents based on choline chloride. *J. Electroanal. Chem.*, **599**, pp. 288–294.
9. Anderson, J. L., Armstrong, D. W., and Wei, G. T. (2006). Ionic liquids in analytical chemistry. *Anal. Chem.*, **78**, pp. 2892–2902.
10. Buehler, G., and Feldmann, C. (2006). Microwave-assisted synthesis of luminescent LaPO<sub>4</sub>: Ce,Tb nanocrystals in ionic liquids. *Angew. Chem. Int. Edit.*, **45**, pp. 4864–4867.
11. Zhou, Y., and Antonietti, M. (2003). Preparation of highly ordered monolithic super-microporous lamellar silica with a room-temperature ionic liquid as template via the nanocasting technique. *Adv. Mater.*, **15**, pp. 1452–1455.
12. Antonietti, M., Kuang, D. B., Smarsly, B., and Zhou, Y. (2004). Ionic liquids for the convenient synthesis of functional nanoparticles

- and other inorganic nanostructures. *Angew. Chem. Int. Ed.*, **43**, pp. 4988–4992.
13. Welton, T. (1999). Room-temperature ionic liquids: solvents for synthesis and catalysis. *Chem. Rev.*, **99**, pp. 2071–2084.
  14. El Seoud, O. A., Koschella, A., Fidale, L. C., Dorn, S., and Heinze, T. (2007). Applications of ionic liquids in carbohydrate chemistry: a window of opportunities. *Biomacromolecules*, **8**, pp. 2629–2647.
  15. Abbott, A. P., Cullis, P. M., Gibson, M. J., Harris, R. C., and Raven, E. (2007). Extraction of glycerol from biodiesel into a eutectic based ionic liquid. *Green Chem.*, **9**, pp. 868–872.
  16. Blanchard, L. A., Hancu, D., Beckman, E. J., and Brennecke, J. F. (1999). Green processing using ionic liquids and CO<sub>2</sub>. *Nature*, **399**, pp. 28–29.
  17. Swatloski, R. P., Visser, A. E., Reichert, W. M., Broker, G. A., Farina, L. M., Holbrey, J. D., and Rogers, R. D. (2002). On the solubilization of water with ethanol in hydrophobic hexafluorophosphate ionic liquids. *Green Chem.*, **4**, pp. 81–87.
  18. Swatloski, R. P., Spear, S. K., Holbrey, J. D., and Rogers, R. D. (2002). Dissolution of cellulose with ionic liquids. *J. Am. Chem. Soc.*, **124**, pp. 4974–4975.
  19. Winterton, N. (2006). Solubilization of polymers by ionic liquids. *J. Mater. Chem.*, **16**, pp. 4281–4293.
  20. Liu, J., Cheng, S., Zhang, J., Feng, X., Fu, X., and Han, B. (2007). Reverse micelles in carbon dioxide with ionic-liquid domains. *Angew. Chem. Int. Ed.*, **46**, pp. 3313–3315.
  21. Miller, A. L., and Bowden, N. B. (2007). Room temperature ionic liquids: new solvents for Schrock's catalyst and removal using polydimethylsiloxane membranes. *Chem. Commun.*, pp. 2051–2053.
  22. Choi, D. S., Kim, J. H., Shin, U. S., Deshmukh, R. R., and Song, C. E. (2007). Thermodynamically- and kinetically-controlled Friedel–Crafts alkenylation of arenes with alkynes using an acidic fluoroantimonate(V) ionic liquid as catalyst. *Chem. Commun.*, pp. 3482–3484.
  23. Mehnert, C. P. (2005). Supported ionic liquid catalysis. *Chem. Eur. J.*, **11**, pp. 50–56.

24. Parvulescu, V. I., and Hardacre, C. (2007). Catalysis in ionic liquids. *Chem. Rev.*, **107**, pp. 2615–2665.
25. Gu, Y. L., Karam, A., Jerome, F., and Barrault, J. (2007). Selectivity enhancement of silica-supported sulfonic acid catalysts in water by coating of ionic liquid. *Org. Lett.*, **9**, pp. 3145–3148.
26. Pringle, J. M., Ngamna, O., Lynam, C., Wallace, G. G., Forsyth, M., and MacFarlane, D. R. (2007). Conducting polymers with fibrillar morphology synthesized in a biphasic ionic liquid/water system. *Macromolecules*, **40**, pp. 2702–2711.
27. Hapiot, P., and Lagrost, C. (2008). Electrochemical reactivity in room-temperature ionic liquids. *Chem. Rev.*, **108**, pp. 2238–2264.
28. Armand, M., Endres, F., MacFarlane, D. R., Ohno, H., and Scrosati, B. (2009). Ionic-liquid materials for the electrochemical challenges of the future. *Nat Mater*, **8**, pp. 621–629.
29. Wei, D., and Ivaska, A. (2008). Applications of ionic liquids in electrochemical sensors. *Anal. Chim. Acta*, **607**, pp. 126–135.
30. Soukup-Hein, R. J., Warnke, M. M., and Armstrong, D. W. (2009). Ionic liquids in analytical chemistry. *Annu. Rev. Anal. Chem.*, **2**, pp. 145–168.
31. Liu, J. F., Jonsson, J. A., and Jiang, G. B. (2005). Application of ionic liquids in analytical chemistry. *TrAC-Trend. Anal. Chem.*, **24**, pp. 20–27.
32. Fukushima, T., Kosaka, A., Ishimura, Y., Yamamoto, T., Takigawa, T., Ishii, N., and Aida, T. (2003). Molecular ordering of organic molten salts triggered by single-walled carbon nanotubes. *Science*, **300**, pp. 2072–2074.
33. Zhang, Y. J., Shen, Y. F., Li, J. H., Niu, L., Dong, S. J., and Ivaska, A. (2005). Electrochemical functionalization of single-walled carbon nanotubes in large quantities at a room-temperature ionic liquid supported three-dimensional network electrode. *Langmuir*, **21**, pp. 4797–4800.
34. Wei, D., Kvarnstrom, C., Lindfors, T., and Ivaska, A. (2007). Electrochemical functionalization of single walled carbon nanotubes with polyaniline in ionic liquids. *Electrochem. Commun.*, **9**, pp. 206–210.

35. El Abedin, S. Z., Polleth, M., Meiss, S. A., Janek, J., and Endres, F. (2007). Ionic liquids as green electrolytes for the electrodeposition of nanomaterials. *Green Chem.*, **9**, pp. 549–553.
36. Lin, Y. W., Tai, C. C., and Sun, I. W. (2007). Electrochemical preparation of porous copper surfaces in zinc chloride-1-ethyl-3-methyl imidazolium chloride ionic liquid. *J. Electrochem. Soc.*, **154**, pp. D316–D321.
37. Moustafa, E. M., El Abedin, S. Z., Shkurankov, A., Zschippang, E., Saad, A. Y., Bund, A., and Endres, F. (2007). Electrodeposition of Al in 1-butyl-1-methylpyrrolidinium bis(trifluoromethylsulfonyl)amide and 1-ethyl-3-methylimidazolium bis(trifluoromethylsulfonyl)amide ionic liquids: In situ STM and EQCM studies. *J. Phys. Chem. B*, **111**, pp. 4693–4704.
38. Mukhopadhyay, I., and Freyland, W. (2003). Electrodeposition of Ti nanowires on highly oriented pyrolytic graphite from an ionic liquid at room temperature. *Langmuir*, **19**, pp. 1951–1953.
39. Yu, P., Yan, J., Zhang, J., and Mao, L. Q. (2007). Cost-effective electrodeposition of platinum nanoparticles with ionic liquid droplet confined onto electrode surface as micro-media. *Electrochem. Commun.*, **9**, pp. 1139–1144.
40. Bhatt, A. I., Mechler, A., Martin, L. L., and Bond, A. M. (2007). Synthesis of Ag and Au nanostructures in an ionic liquid: thermodynamic and kinetic effects underlying nanoparticle, cluster and nanowire formation. *J. Mater. Chem.*, **17**, pp. 2241–2250.
41. Jia, F. L., Yu, C. F., Deng, K. J., and Zhang, L. H. (2007). Nanoporous metal (Cu, Ag, Au) films with high surface area: General fabrication and preliminary electrochemical performance. *J. Phys. Chem. C*, **111**, pp. 8424–8431.
42. Oyama, T., Okajima, T., and Ohsaka, T. (2007). Electrodeposition of gold at glassy carbon electrodes in room-temperature ionic liquids. *J. Electrochem. Soc.*, **154**, pp. D322–D327.
43. Borisenko, N., Zein El Abedin, S., and Endres, F. (2006). In situ STM investigation of gold reconstruction and of silicon electrodeposition on Au(111) in the room temperature ionic liquid 1-butyl-1-methylpyrrolidinium bis(trifluoromethylsulfonyl)imide. *J. Phys. Chem. B*, **110**, pp. 6250–6256.

44. Mehnert, C. P., Cook, R. A., Dispenziere, N. C., and Afeworki, M. (2002). Supported ionic liquid catalysis — a new concept for homogeneous hydroformylation catalysis. *J. Am. Chem. Soc.*, **124**, pp. 12932–12933.
45. Gadenne, B., Hesemann, P., and Moreau, J. J. E. (2004). Supported ionic liquids: ordered mesoporous silicas containing covalently linked ionic species. *Chem. Comm.*, pp. 1768–1769.
46. Lee, B. S., Chi, Y. S., Lee, J. K., Choi, I. S., Song, C. E., Namgoong, S. K., and Lee, S.-g. (2004). Imidazolium ion-terminated self-assembled monolayers on Au: effects of counteranions on surface wettability. *J. Am. Chem. Soc.*, **126**, pp. 480–481.
47. Choi, E. Y., Azzaroni, O., Cheng, N., Zhou, F., Kelby, T., and Huck, W. T. S. (2007). Electrochemical characteristics of polyelectrolyte brushes with electroactive counterions. *Langmuir*, **23**, pp. 10389–10394.
48. Yu, P., Lin, Y., Xiang, L., Su, L., Zhang, J., and Mao, L. (2005). Molecular films of water-miscible ionic liquids formed on glassy carbon electrodes: characterization and electrochemical applications. *Langmuir*, **21**, pp. 9000–9006.
49. Zhao, F., Wu, X., Wang, M. K., Liu, Y., Gao, L. X., and Dong, S. J. (2004). Electrochemical and bioelectrochemistry properties of room-temperature ionic liquids and carbon composite materials. *Anal. Chem.*, **76**, pp. 4960–4967.
50. Shen, Y. F., Zhang, Y. J., Zhang, Q. X., Niu, L., You, T. Y., and Ivaska, A. (2005). Immobilization of ionic liquid with polyelectrolyte as carrier. *Chem. Commun.*, pp. 4193–4195.
51. Li, F., Shan, C., Bu, X., Shen, Y., Yang, G., and Niu, L. (2008). Fabrication and electrochemical characterization of electrostatic assembly of polyelectrolyte-functionalized ionic liquid and Prussian blue ultrathin films. *J. Electroanal. Chem.*, **616**, pp. 1–6.
52. Yang, F., Jiao, L., Shen, Y., Xu, X., Zhang, Y., and Niu, L. (2007). Enhanced response induced by polyelectrolyte-functionalized ionic liquid in glucose biosensor based on sol-gel organic-inorganic hybrid material. *J. Electroanal. Chem.*, **608**, pp. 78–83.
53. Shen, Y. F., Zhang, Y. J., Qiu, X. P., Guo, H. Q., Niu, L., and A., I. (2007). Polyelectrolyte-functionalized ionic liquid for electrochemistry in

- supporting electrolyte-free aqueous solutions and application in amperometric flow injection analysis. *Green Chem.*, **9**, pp. 746–753.
54. Han, D., Qiu, X., Shen, Y., Guo, H., Zhang, Y., and Niu, L. (2006). Electropolymerization of polypyrrole on PFIL-PSS-modified electrodes without added support electrolytes. *J. Electroanal. Chem.*, **596**, pp. 33–37.
  55. Wei, D., Unalan, H. E., Han, D. X., Zhang, Q. X., Niu, L., Amaratunga, G., and Ryhanen, T. (2008). A solid-state dye-sensitized solar cell based on a novel ionic liquid gel and ZnO nanoparticles on a flexible polymer substrate. *Nanotechnology*, **19**, pp. 424006–424010.
  56. Zhang, Y. J., Shen, Y. F., Yuan, J. H., Han, D. X., Wang, Z. J., Zhang, Q. X., and Niu, L. (2006). Design and synthesis of multifunctional materials based on an ionic-liquid backbone. *Angew. Chem. Int. Edit.*, **45**, pp. 5867–5870.
  57. Yu, B., Zhou, F., Liu, G., Liang, Y., Huck, W. T. S., and Liu, W. M. (2006). The electrolyte switchable solubility of multi-walled carbon nanotube/ionic liquid (MWCNT/IL) hybrids. *Chem. Commun.*, pp. 2356–2358.
  58. Zhang, Y. J., Shen, Y. F., Kuehner, D., Wu, S. X., Su, Z. M., Ye, S., and Niu, L. (2008). Directing single-walled carbon nanotubes to self-assemble at water/oil interfaces and facilitate electron transfer. *Chem. Commun.*, pp. 4273–4275.
  59. Zhang, Y., Shen, Y., Han, D., Wang, Z., Song, J., Li, F., and Niu, L. (2007). Carbon nanotubes and glucose oxidase bionanocomposite bridged by ionic liquid-like unit: Preparation and electrochemical properties. *Biosens. Bioelectron.*, **23**, pp. 438–443.
  60. Shan, C., Yang, H., Song, J., Han, D., Ivaska, A., and Niu, L. (2009). Direct electrochemistry of glucose oxidase and biosensing for glucose based on graphene. *Anal Chem*, **81**, pp. 2378–2382.
  61. Wang, Z., Zhang, Q., Kuehner, D., Xu, X., Ivaska, A., and Niu, L. (2008). The synthesis of ionic-liquid-functionalized multiwalled carbon nanotubes decorated with highly dispersed Au nanoparticles and their use in oxygen reduction by electrocatalysis. *Carbon*, **46**, pp. 1687–1692.
  62. Wu, B. H., Hu, D., Kuang, Y. J., Liu, B., Zhang, X. H., and Chen, J. H. (2009). Functionalization of carbon nanotubes by an ionic-liquid polymer:

- dispersion of Pt and PtRu nanoparticles on carbon nanotubes and their electrocatalytic oxidation of methanol. *Angew. Chem. Int. Edit.*, **48**, pp. 4751–4754.
63. Wang, Z. J., Zhang, Q. X., Kuehner, D., Ivaska, A., and Niu, L. (2008). Green synthesis of 1–2 nm gold nanoparticles stabilized by amine-terminated ionic liquid and their electrocatalytic activity in oxygen reduction. *Green Chem.*, **10**, pp. 907–909.
  64. Li, F. H., Yang, H. F., Shan, C. S., Zhang, Q. X., Han, D. X., Ivaska, A., and Niu, L. (2009). The synthesis of perylene-coated graphene sheets decorated with Au nanoparticles and its electrocatalysis toward oxygen reduction. *J. Mater. Chem.*, **19**, pp. 4022–4025.
  65. Li, F. H., Wang, Z. H., Shan, C. S., Song, J. F., Han, D. X., and Niu, L. (2009). Preparation of gold nanoparticles/functionalized multiwalled carbon nanotube nanocomposites and its glucose biosensing application. *Biosens. Bioelectron.*, **24**, pp. 1765–1770.
  66. Li, F. H., Li, F., Song, J. X., Song, J. F., Han, D. X., and Niu, L. (2009). Green synthesis of highly stable platinum nanoparticles stabilized by amino-terminated ionic liquid and its electrocatalysts for dioxygen reduction and methanol oxidation. *Electrochem. Commun.*, **11**, pp. 351–354.
  67. Yang, H. F., Shan, C. S., Li, F. H., Han, D. X., Zhang, Q. X., and Niu, L. (2009). Covalent functionalization of polydisperse chemically-converted graphene sheets with amine-terminated ionic liquid. *Chem. Commun.*, pp. 3880–3882.
  68. Shan, C. S., Li, F. H., Yuan, F. Y., Yang, G. F., Niu, L., and Zhang, Q. (2008). Size-controlled synthesis of monodispersed gold nanoparticles stabilized by polyelectrolyte-functionalized ionic liquid. *Nanotechnology*, **19**, pp. 285601–285606.
  69. Jia, F., Shan, C., Li, F., and Niu, L. (2008). Carbon nanotube/gold nanoparticles/polyethylenimine-functionalized ionic liquid thin film composites for glucose biosensing. *Biosens. Bioelectron.*, **24**, pp. 951–956.
  70. Azzaroni, O., Brown, A. A., Cheng, N., Wei, A., Jonas, A. M., and Huck, W. T. S. (2007). Synthesis of gold nanoparticles inside polyelectrolyte brushes. *J. Mater. Chem.*, **17**, pp. 3433–3439.
  71. Shen, Y. F., Zhang, Y. J., Kuehner, D., Yang, G. F., Yuan, F. Y., and Niu, L. (2008). Ion-responsive behavior of ionic-liquid surfactant

- aggregates with applications in controlled release and emulsification. *Chemphyschem*, **9**, pp. 2198–2202.
72. Shen, Y., Zhang, Y., Han, D., Wang, Z., Kuehner, D., and Niu, L. (2009). Preparation of colorless ionic liquids “on water” for spectroscopy. *Talanta*, **78**, pp. 805–808.